Helmholtz-Hodge Decomposition on $[0,1]^d$ by Divergence-free and Curl-free Wavelets

Souleymane Kadri Harouna* and Valérie Perrier *

Springer-Verlag, Computer Science Editorial,
Tiergartenstr. 17, 69121 Heidelberg, Germany
{Souleymane.Kadri-Harouna@imag.fr,Valerie.Perrier@imag.fr}
http://www.springer.com/lncs

Abstract. *This paper deals with the Helmholtz-Hodge decomposition of a vector field in bounded domain. We present a practical algorithm to compute this decomposition in the context of divergence-free and curl-free wavelets satisfying suitable boundary conditions. The method requires the inversion of divergence-free and curl-free wavelet Gram matrices. We propose an optimal preconditioning which allows to solve the systems with a small number of iterations. Finally, numerical examples prove the accuracy and the efficiency of the method.*

Keywords: Divergence-free and curl-free wavelets; Helmholtz-Hodge decomposition.

1 Introduction

Vector field analysis is ubiquitous in engineering, physics or applied mathematics. Most of the solutions of problems arising from these domains are vector fields and they have some compatibility properties related to the nature of the problem. This is the case in the numerical simulation of incompressible fluid flows where the velocity field is divergence-free or in electromagnetism where the electric field contained in the electromagnetic field is curl-free.

The Helmholtz-Hodge decomposition, under certain smoothness assumptions, allows to separate any vector field into the sum of three uniquely defined components: divergence-free, curl-free and gradient of a harmonic function. Thus, the Helmholtz-Hodge decomposition provides a powerful tool for several applications such as the resolution of partial differential equations [14], aerodynamic design [25], detection of flow features [22] or computer graphics [21]. Therefore, it is important to have at hand an efficient algorithm to deal with such decomposition numerically.

In case of periodic boundary conditions, Fourier domain offers an ideal setting to compute the Helmholtz-Hodge decomposition, thanks to the Leray projector

* Laboratoire Jean Kuntzmann, University of Grenoble, BP 53 Grenoble Cedex 9, France

which writes explicitly [11]. For more general (physical) boundary conditions, this decomposition is usually achieved by solving a Poisson equation relative to each field component: this is the case when using finite element or finite difference methods [14]. The well known drawback of these methods is their cost, for example in particle-based physical simulations. Then, one resorts to mesh-less method [21] or methods leading to variational equations [22].

In the wavelet setting the Helmholtz-Hodge decomposition will not use the resolution of a Poisson equation, since one knows explicit bases for the divergence-free and curl-free function spaces [12,13,19,26]. In this context, Urban [27], and latter Deriaz and Perrier [11] introduced methods to compute the orthogonal projections onto divergence-free and curl-free wavelet bases. These wavelet methods provide accuracy for a small number of degrees of freedom, due to the good non-linear approximation property provided by wavelet bases [7]. However, the works of [11,27] were limited to periodic boundary conditions for lack of suitable bases.

The main objective of this paper is to extend the works of [11,27] to more general physical boundary conditions. We first recall the principles of the tensor-product divergence-free and curl-free wavelet construction on the cube, that was detailed in [18] for the 2D case (see also [17]). Similar constructions, leading to different bases, were proposed by Stevenson in general dimension [23,24]. Then we propose an effective method for the Helmholtz-Hodge decomposition based on the computation and inversion of corresponding Gram matrices. The tensor structure of the bases is fully exploited to reduce the computational complexity. Moreover the system is solved with a low complexity, thanks to an optimal preconditioning.

The layout of this paper is as follows. In section 2, we recall the theoretical definition and mathematical background of the Helmholtz-Hodge decomposition on a bounded domain of $\mathbb{R}^d$. In section 3 we explicit the construction of divergence-free and curl-free wavelets on $[0,1]^d$ with desired boundary conditions. Section 4 is devoted to the description of the numerical method for the Helmholtz-Hodge decomposition, and numerical examples will illustrate its performance.

2 Helmholtz-Hodge decomposition

We recall in this section some definitions related to the Helmholtz-Hodge decomposition on a bounded Lipschitz domain Ω of $\mathbb{R}^d$ [14]. We assume that the domain Ω and its boundary Γ have sufficient regularities (see [1,14]).

2.1 Definitions

The Helmholtz-Hodge decomposition theorem [6,14] states that any vector field $\mathbf{u} \in (L^2(\Omega))^d$ can be uniquely decomposed into the sum of its divergence-free,

curl-free and gradient of harmonic function components:

$$\mathbf{u} = \mathbf{u}_{\text{div}} + \mathbf{u}_{\text{curl}} + \mathbf{u}_{\text{har}} \tag{1}$$

with:

$$\nabla \cdot \mathbf{u}_{\text{div}} = 0 \qquad \text{and} \qquad \nabla \times \mathbf{u}_{\text{curl}} = 0 \tag{2}$$

The last component $\mathbf{u}_{\text{har}}$ is both divergence-free and irrotational:

$$\nabla \cdot \mathbf{u}_{\text{har}} = 0 \qquad \text{and} \qquad \nabla \times \mathbf{u}_{\text{har}} = 0 \tag{3}$$

Following [1,14], this decomposition may alternatively be written using scalar potentials. There exist a scalar potential $q \in H_0^1(\Omega)$ and a harmonic potential $h \in H^1(\Omega)$ such as:

$$\mathbf{u}_{\text{curl}} = \nabla q \qquad \text{and} \qquad \mathbf{u}_{\text{har}} = \nabla h$$

Moreover, the scalars q and h are uniquely defined.

In terms of spaces, the decomposition (1) corresponds to an orthogonal splitting of $(L^2(\Omega))^d$:

$$(L^2(\Omega))^d = \mathcal{H}_{div}(\Omega) \oplus \mathcal{H}_{curl}(\Omega) \oplus \mathcal{H}_{har}(\Omega) \tag{4}$$

where $\mathcal{H}_{div}(\Omega)$ is the space of divergence-free vector functions of $(L^2(\Omega))^d$ with vanishing normal boundary condition:

$$\mathcal{H}_{div}(\Omega) = \{\mathbf{u} \in (L^2(\Omega))^d : \ \mathbf{div}(\mathbf{u}) = 0, \ \mathbf{u} \cdot \mathbf{n}|_\Gamma = 0\} \tag{5}$$

For $d = 2, 3$, the space $\mathcal{H}_{div}(\Omega)$ coincides with the *curl of potential* space (see [1,2,14]):

$$\mathcal{H}_{div}(\Omega) = \{\mathbf{u} = \mathbf{curl}(\mathbf{\Psi}) : \mathbf{\Psi} \in (H_0^1(\Omega))^d\}, \qquad (\mathbf{\Psi} \in H_0^1(\Omega) \ \text{ if } \ d = 2) \tag{6}$$

In this case, the component $\mathbf{u}_{\text{div}}$ of (1) reads: $\mathbf{u}_{\text{div}} = \mathbf{curl}(\mathbf{\Psi})$

On the other hand, the space $\mathcal{H}_{curl}$ corresponds to the gradient of $H^1(\Omega)$-potentials which vanish on Γ:

$$\mathcal{H}_{curl}(\Omega) = \{\mathbf{u} = \nabla q : \ q \in H_0^1(\Omega)\} \tag{7}$$

Finally, $\mathcal{H}_{har}$ corresponds to the gradient of $H^1(\Omega)$-harmonic potentials:

$$\mathcal{H}_{har}(\Omega) = \{\mathbf{u} = \nabla h : \ h \in H^1(\Omega), \ \Delta h = 0\} \tag{8}$$

Other splittings exist, for example in $(H_0^1(\Omega))^d$ to incorporate homogeneous boundary conditions [14].

In the whole space $\mathbb{R}^d$ or with periodic boundary conditions, the decomposition (1) is explicit in Fourier domain and the third term vanishes: $\mathbf{u}_{\text{har}} = 0$ (one obtains the Helmholtz decomposition in this case [11,27]). In the wavelet context, an iterative procedure was proposed by Deriaz and Perrier [11]. The purpose here is to extend such method with boundary conditions for the spaces $\mathcal{H}_{div}(\Omega)$, $\mathcal{H}_{curl}(\Omega)$ and $\mathcal{H}_{har}(\Omega)$ introduced in (5, 7, 8).

3 Divergence-free and curl-free wavelets on $[0,1]^d$

This section introduces the principles of the construction and main properties of divergence-free and curl-free wavelets on the hypercube $[0,1]^d$. The two dimensional case $d = 2$ has been detailed in [18], with explicit examples (spline, Daubechies wavelets), and practical tools for the implementation (filters, fast wavelet transform, ..). We develop below the extension to more general dimensions $d \geq 3$. Recently, Stevenson proposed a first construction [23,24], which led to alternative wavelet bases. A first advantage of our construction is that it fits perfectly with the classical multiresolution analysis construction on the interval $[0,1]$.

The construction is based on 1D multiresolution analysis generators $(\varphi^1, \tilde{\varphi}^1)$ and $(\varphi^0, \tilde{\varphi}^0)$ linked by differentiation / integration, and introduced by Lemarié-Rieusset and collaborators in original works [16,19]. It follows two steps, described in the two forthcoming sections:

(i) Construction of two biorthogonal MRAs of $L^2(0,1)$ linked by differentiation / integration.

(ii) Construction of MRAs and wavelet bases of $\mathcal{H}_{div}(\Omega)$ and $\mathcal{H}_{curl}(\Omega)$.

3.1 Multiresolution analyses of $L^2(0,1)$ linked by differentiation / integration

The construction of regular biorthogonal multiresolution analyses (BMRA) on the interval $[0,1]$ is now classical (see [5,9,15,20]). It begins with a pair of biorthogonal compactly supported scaling functions $(\varphi^1, \tilde{\varphi}^1)$ [8] of $L^2(\mathbb{R})$, with some r polynomial reproduction:

$$x^\ell = \sum_{k\in\mathbb{Z}} \langle x^\ell, \tilde{\varphi}^1(x-k)\rangle \ \varphi^1(x-k) \qquad \text{for} \qquad 0 \leq \ell \leq r-1 \tag{9}$$

and similarly for $\tilde{\varphi}^1$, with $\tilde{r}$ polynomial reproduction.

Following classical constructions, one defines finite dimensional biorthogonal multiresolution spaces:

$$V_j^1 = \text{span}\{\varphi_{j,k}^1 \ ; \ 0 \leq k \leq N_j - 1\} \ \text{ and } \ \tilde{V}_j^1 = \text{span}\{\tilde{\varphi}_{j,k}^1 \ ; \ 0 \leq k \leq N_j - 1\} \tag{10}$$

whose dimension $N_j \simeq 2^j$ depends on some *free* integer parameters (δ_0, δ_1). The scaling functions $\varphi_{j,k}^1$ satisfy $\varphi_{j,k}^1 = 2^{j/2}\varphi^1(2^j x - k)$ "inside" the interval $[0,1]$, but this is no more true near the boundaries 0 and 1 (idem for $\tilde{\varphi}_{j,k}^1$). In practice, the scale index j must be great than some index j_{min}, to avoid boundary effects. The biorthogonality between bases writes: $< \varphi_{j,k}^1 / \tilde{\varphi}_{j,k'}^1 >= \delta_{k,k'}$
The approximation order provided by such MRA (V_j^1) in $L^2(0,1)$ is r:

$$\forall \ f \in H^s(0,1), \quad \inf_{f_j \in V_j^1} \|f - f_j\|_{L^2(0,1)} \leq C 2^{-js}, \quad 0 \leq s \leq r \tag{11}$$

whereas $(\tilde{V}_j^1)$ has for approximation order $\tilde{r}$.

Homogeneous Dirichlet boundary conditions can be simply imposed on (V_j^1) by removing one scaling function at each boundary 0 and 1:

$$V_j^D = V_j^1 \cap H_0^1(0,1) = \text{span}\{\varphi_{j,k}^1 \ ; \ 1 \leq k \leq N_j - 2\} \tag{12}$$

A possibility to adjust the dimension of the two biorthogonal spaces $(V_j^D, \tilde{V}_j^D)$ is to impose $\tilde{V}_j^D = \tilde{V}_j^1 \cap H_0^1(0,1)$, and $\tilde{V}_j^D$ rewrites (keeping the same notation for the basis functions, which have changed after biorthogonalization):

$$\tilde{V}_j^D = \text{span}\{\tilde{\varphi}_{j,k}^1 \ ; \ 1 \leq k \leq N_j - 2\} \tag{13}$$

As usual, biorthogonal wavelet spaces $(W_j^1, \tilde{W}_j^1)$ are defined by:

$$W_j^1 = V_{j+1}^1 \cap (\tilde{V}_j^1)^\perp \qquad\qquad \tilde{W}_j^1 = \tilde{V}_{j+1}^1 \cap (V_j^1)^\perp \tag{14}$$

and generated by finite dimensional wavelet bases on the interval [15,20]:

$$W_j^1 = \text{span}\{\psi_{j,k}^1 \ ; \ 0 \leq k \leq 2^j - 1\} \ \text{ and } \ \tilde{W}_j^1 = \text{span}\{\tilde{\psi}_{j,k}^1 \ ; \ 0 \leq k \leq 2^j - 1\} \tag{15}$$

The difficulty now is to derive a new biorthogonal MRA $(V_j^0, \tilde{V}_j^0)$ of $L^2(0,1)$ such that:

$$\frac{d}{dx} V_j^1 = V_j^0$$

The existence of such biorthogonal MRA was already proved by Jouini and Lemarié-Rieusset [16] and it should be based on generators $(\varphi^0, \tilde{\varphi}^0)$ introduced in [19] satisfying:

$$(\varphi^1(x))' \ = \ \varphi^0(x) - \varphi^0(x-1) \qquad \text{and} \qquad (\tilde{\varphi}^0(x))' \ = \ \tilde{\varphi}^1(x+1) - \tilde{\varphi}^1(x) \tag{16}$$

Let us introduce the primitive space for $\tilde{V}_j^1$:

$$\int_0^x \tilde{V}_j^1 = \{g \ : \exists \ f \in \tilde{V}_j^1 \text{ such that } g(x) = \int_0^x f(t)dt\}$$

In [18], we proposed a practical construction of spaces $(V_j^0, \tilde{V}_j^0)$:

$$V_j^0 = \text{span}\{\varphi_{j,k}^0 \ ; \ 0 \leq k \leq N_j - 2\} \ \text{ and } \ \tilde{V}_j^0 = \text{span}\{\tilde{\varphi}_{j,k}^0 \ ; \ 0 \leq k \leq N_j - 2\} \tag{17}$$

different from the underlying spaces of [24], but satisfying the following proposition.

Proposition 1.
The two BMRAs $(V_j^\epsilon, \tilde{V}_j^\epsilon)_{\epsilon=0,1}$ *of* $L^2(0,1)$ *constructed in [18] from biorthogonal generators* $(\varphi^\epsilon, \tilde{\varphi}^\epsilon)_{\epsilon=0,1}$ *satisfying relation* (16)*, verify :*

$$(i)\ \frac{d}{dx}V_j^1 = V_j^0 \quad and \quad \frac{d}{dx}\circ\mathcal{P}_j^1 f = \mathcal{P}_j^0 \circ \frac{d}{dx}f, \quad \forall\ f \in H^1(0,1)$$

$$(ii)\ \tilde{V}_j^0 = H_0^1(0,1) \cap \int_0^x \tilde{V}_j^1 \quad and \quad \frac{d}{dx}\circ\tilde{\mathcal{P}}_j^0 f = \tilde{\mathcal{P}}_j^1 \circ \frac{d}{dx}f, \quad \forall\ f \in H_0^1(0,1)$$

where $(\mathcal{P}_j^\epsilon, \tilde{\mathcal{P}}_j^\epsilon)$ *are the biorthogonal projectors on* $(V_j^\epsilon, \tilde{V}_j^\epsilon)$.

Wavelet bases of the biorthogonal MRA $(V_j^0, \tilde{V}_j^0)_{j\geq j_{min}}$ are simply defined by respectively differentiating and integrating the wavelets of $(V_j^1, \tilde{V}_j^1)_{j\geq j_{min}}$, as stated by the following proposition [16,18].

Proposition 2. *[16,18]*
Let $\{\psi_{j,k}^1\}$ *and* $\{\tilde{\psi}_{j,k}^1\}$ *be biorthogonal wavelet bases of respectively* W_j^1 *and* $\tilde{W}_j^1$*. Then, the wavelets defined by:*

$$\psi_{j,k}^0 = 2^{-j}(\psi_{j,k}^1)' \qquad and \qquad \tilde{\psi}_{j,k}^0 = -2^j \int_0^x \tilde{\psi}_{j,k}^1 \tag{18}$$

are respectively biorthogonal wavelet bases of W_j^0 *and* $\tilde{W}_j^0$*:*

$$W_j^0 = V_{j+1}^0 \cap (\tilde{V}_j^0)^\perp \qquad and \qquad \tilde{W}_j^0 = \tilde{V}_{j+1}^0 \cap (V_j^0)^\perp \tag{19}$$

Remark 1.
The wavelets $\psi_{j,k}^0$ and $\tilde{\psi}_{j,k}^0$ defined by (18) differ from the standard wavelet construction [5,9,20] in BMRA $(V_j^0, \tilde{V}_j^0)$: indeed, the usual wavelets on the interval do not lead to the differentiation/integration relation (18), except for interior wavelets.

3.2 Divergence-free scaling functions and wavelets on $[0,1]^d$

Le Ω be the hypercube $\Omega = [0,1]^d$. The objective in this section is to derive wavelet bases of the space $\mathcal{H}_{div}(\Omega)$, with vanishing outward normal at the boundary $\Gamma = \partial\Omega$. Following (5), $\mathcal{H}_{div}(\Omega)$ is the curl of the space $H_0^1(\Omega)$ $(d=2)$ or $(H_0^1(\Omega))^d$ $(d=3)$ of scalar (vector for $d=3$) stream functions [1]. We begin with the description of basis functions in the 2D case (already detailed in [18]), then we propose a generalization of the construction for $d \geq 3$.

Two-dimensional case:
We start with the 2D MRA $(V_j^D \otimes V_j^D)_{j\geq j_{min}}$ of $H_0^1(\Omega)$, where $(V_j^D)_{j\geq j_{min}}$ is the 1D MRA of $H_0^1(0,1)$ defined in section 3.1 (12). For each scale index $j \geq j_{min}$,

divergence-free scaling functions on $\Omega = [0,1]^2$ are constructed by taking the curl of scaling functions of $V_j^D \otimes V_j^D$:

$$\Phi_{j,\mathbf{k}}^{div} := \mathbf{curl}[\varphi_{j,k_1}^D \otimes \varphi_{j,k_2}^D] = \begin{vmatrix} \varphi_{j,k_1}^D \otimes (\varphi_{j,k_2}^D)' \\ -(\varphi_{j,k_1}^D)' \otimes \varphi_{j,k_2}^D \end{vmatrix}, \quad 1 \le k_1, k_2 \le N_j - 2 \tag{20}$$

The choice of space V_j^D ensures that the divergence-free scaling functions satisfy the boundary condition $\Phi_{j,\mathbf{k}}^{div} \cdot \mathbf{n} = 0$ by construction. Let $\mathbf{V}_j^{div}$ be the space spanned by these divergence-free scaling functions:

$$\mathbf{V}_j^{div} = \text{span}\{\Phi_{j,\mathbf{k}}^{div}\}, \quad 1 \le k_1, k_2 \le N_j - 2 \tag{21}$$

By construction, the spaces $\mathbf{V}_j^{div}$ form a multiresolution analysis of $\mathcal{H}_{div}(\Omega)$, since it can be proven from proposition 1 that we have [18]:

$$\mathbf{V}_j^{div} = (V_j^D \otimes V_j^0) \times (V_j^0 \otimes V_j^D) \cap \mathcal{H}_{div}(\Omega) \tag{22}$$

In the same manner, the corresponding anisotropic divergence-free wavelets on Ω are defined by taking the curl of the three types of scalar anisotropic wavelets associated to $V_j^D \otimes V_j^D$: for $\mathbf{j} = (j_1, j_2)$, with $j_1, j_2 > j_{min}$,

$$\begin{aligned}
\Psi_{\mathbf{j},\mathbf{k}}^{div,1} &:= \mathbf{curl}[\varphi_{j_{min},k}^D \otimes \psi_{j_2,k_2}^D],\ 1 \le k \le N_{j_{min}} - 2,\ \ 0 \le k_2 \le 2^{j_2} - 1 \\
\Psi_{\mathbf{j},\mathbf{k}}^{div,2} &:= \mathbf{curl}[\psi_{j_1,k_1}^D \otimes \varphi_{j_{min},k}^D],\ 0 \le k_1 \le 2^{j_1} - 1,\ \ 1 \le k \le N_{j_{min}} - 2 \\
\Psi_{\mathbf{j},\mathbf{k}}^{div,3} &:= \mathbf{curl}[\psi_{j_1,k_1}^D \otimes \psi_{j_2,k_2}^D],\ \ 0 \le k_1 \le 2^{j_1} - 1,\ 0 \le k_2 \le 2^{j_2} - 1
\end{aligned}$$

$(\psi_{j,k}^D)$ being the wavelet basis of $W_j^D = V_{j+1}^D \cap (\tilde{V}_j^D)^{\perp}$.

Three-dimensional case:
Divergence-free scaling functions and wavelets on $\Omega = [0,1]^3$ are constructed by taking the curl of suitable scaling functions and wavelets of $(H^1(\Omega))^3$ [1,14]. We will focus on the scaling function construction, since the same technique is used for wavelets. The divergence-free scaling functions are defined by:

$$\Phi_{1,j,\mathbf{k}}^{div} := \mathbf{curl} \begin{vmatrix} 0 \\ 0 \\ \varphi_{j,k_1}^D \otimes \varphi_{j,k_2}^D \otimes \varphi_{j,k_3}^0 \end{vmatrix} = \begin{vmatrix} \varphi_{j,k_1}^D \otimes (\varphi_{j,k_2}^D)' \otimes \varphi_{j,k_3}^0 \\ -(\varphi_{j,k_1}^D)' \otimes \varphi_{j,k_2}^D \otimes \varphi_{j,k_3}^0 \\ 0 \end{vmatrix} \tag{23}$$

$$\Phi_{2,j,\mathbf{k}}^{div} := \mathbf{curl} \begin{vmatrix} \varphi_{j,k_1}^0 \otimes \varphi_{j,k_2}^D \otimes \varphi_{j,k_3}^D \\ 0 \\ 0 \end{vmatrix} = \begin{vmatrix} 0 \\ \varphi_{j,k_1}^0 \otimes \varphi_{j,k_2}^D \otimes (\varphi_{j,k_3}^D)' \\ -\varphi_{j,k_1}^0 \otimes (\varphi_{j,k_2}^D)' \otimes \varphi_{j,k_3}^D \end{vmatrix} \tag{24}$$

$$\Phi_{3,j,\mathbf{k}}^{div} := \mathbf{curl} \begin{vmatrix} 0 \\ \varphi_{j,k_1}^D \otimes \varphi_{j,k_2}^0 \otimes \varphi_{j,k_3}^D \\ 0 \end{vmatrix} = \begin{vmatrix} -\varphi_{j,k_1}^D \otimes \varphi_{j,k_2}^0 \otimes (\varphi_{j,k_3}^D)' \\ 0 \\ (\varphi_{j,k_1}^D)' \otimes \varphi_{j,k_2}^0 \otimes \varphi_{j,k_3}^D \end{vmatrix} \tag{25}$$

These functions are contained in $\mathcal{H}_{div}(\Omega)$ by construction. Let $\mathbf{V}_j^{div}$ be the space spanned by this family: $\mathbf{V}_j^{div} = span\{\Phi_{1,j,\mathbf{k}}^{div}, \Phi_{2,j,\mathbf{k}}^{div}, \Phi_{3,j,\mathbf{k}}^{div}\}$.
Since $\mathcal{H}_{div}(\Omega) = curl(H_0^1(\Omega))^3$, $\mathbf{V}_j^{div}$ is no more than the intersection of the following standard BMRA of $(L^2(\Omega))^3$:

$$\mathbf{V}_j = \left(V_j^1 \otimes V_j^0 \otimes V_j^0\right) \times \left(V_j^0 \otimes V_j^1 \otimes V_j^0\right) \times \left(V_j^0 \otimes V_j^0 \otimes V_j^1\right) \tag{26}$$

with $\mathcal{H}_{div}(\Omega)$.
To each scaling function, we can associate 7 types of anisotropic divergence-free generating wavelets by taking respectively the curl of wavelets of $\{0\} \times \{0\} \times (V_j^D \otimes V_j^D \otimes V_j^0)$, $(V_j^0 \otimes V_j^D \otimes V_j^D) \times \{0\} \times \{0\}$ and $\{0\} \times (V_j^D \otimes V_j^0 \otimes V_j^D) \times \{0\}$, among which we can extract a wavelet basis.

The construction may extend to larger dimensions $d \geq 3$ in the same way. As in the isotropic construction of Lemarié-Rieusset [19], we obtain in this case d types of divergence-free scaling functions For $1 \leq i \leq d$, the general formula of these scaling functions is given by:

$$\Phi_{i,j,\mathbf{k}}^{div} := \begin{array}{c} \\ \text{row } i \ \rightarrow \\ \text{row } i+1 \rightarrow \\ \\ \\ \\ \\ \\ \end{array} \left| \begin{array}{l} 0 \\ \vdots \\ 0 \\ \varphi_{j,k_1}^0 \otimes \cdots \otimes \varphi_{j,k_{i-1}}^0 \otimes \varphi_{j,k_i}^D \otimes (\varphi_{j,k_{i+1}}^D)' \otimes \cdots \otimes \varphi_{j,k_d}^0 \\ -\varphi_{j,k_1}^0 \otimes \cdots \otimes (\varphi_{j,k_i}^D)' \otimes \varphi_{j,k_{i+1}}^D \otimes \varphi_{j,k_{i+2}}^0 \otimes \cdots \otimes \varphi_{j,k_d}^0 \\ 0 \\ \vdots \\ 0 \end{array} \right. \tag{27}$$

(for $i = d$, replace row $i+1$ by row d). These scaling functions $\Phi_{i,j,\mathbf{k}}^{div}$ satisfy the boundary condition : $\Phi_{i,j,\mathbf{k}}^{div} \cdot \mathbf{n} = 0$, by construction. The space $\mathbf{V}_j^{div}$ spanned by this family is included into the following vector-valued multiresolution analysis of $(L^2(\Omega))^d$:

$$\mathbf{V}_j = V_j^{(1)} \times \cdots \times V_j^{(d)} \quad \text{with} \quad V_j^{(i)} = V_j^{\delta_{1,i}} \otimes \cdots \otimes V_j^{\delta_{d,i}}, \ \ 1 \leq i \leq d \tag{28}$$

where $\delta_{j,i}$ denotes the Kronecker symbol. The corresponding wavelet family, generated by the $d(2^d - 1)$ types of corresponding divergence-free wavelets, constitutes an alternative family to the basis built in Stevenson's work [24].

3.3 Curl-free scaling functions and wavelets on $[0, 1]^d$

The construction of irrotational scaling functions and wavelets is easier than in the case of divergence-free functions, since it does not depend on the dimension d. According to the definition (7) of $\mathcal{H}_{curl}(\Omega)$, basis functions will be constructed by taking the gradient of scaling functions and wavelets of a multiresolution analysis of $H_0^1(\Omega)$.

The starting point is again a regular multiresolution analysis of $H_0^1(\Omega)$ given by d tensor-product of V_j^D:

$$\mathbf{V}_j = V_j^D \otimes \cdots \otimes V_j^D \tag{29}$$

Then, the curl-free scaling functions of $\mathcal{H}_{curl}(\Omega)$ are defined by:

$$\Phi_{j,\mathbf{k}}^{\nabla} = \nabla[\varphi_{j,k_1}^D \otimes \cdots \otimes \varphi_{j,k_d}^D] \qquad \text{and} \qquad \mathbf{V}_j^{\nabla} = \text{span}\{\Phi_{j,\mathbf{k}}^{\nabla}\} \tag{30}$$

where $1 \leq k_i \leq N_j - 2$ for $1 \leq i \leq d$. By construction we have:

$$\mathbf{V}_j^{\nabla} = \nabla[V_j^D \otimes \cdots \otimes V_j^D]$$

The multiresolution decomposition of the space $\mathbf{V}_j^{\nabla}$ leads to:

$$\mathbf{V}_j^{\nabla} = \nabla \left[V_{j_{min}}^D \otimes \cdots \otimes V_{j_{min}}^D \bigoplus_{j_{min} \leq j_i \leq j-1} \left(\sum_{\omega \in \Omega_d^*} W_{\mathbf{j}}^{\omega} \right) \right], \quad 1 \leq i \leq d \tag{31}$$

with:

$$\Omega_d^* = \{0,1\}^d \setminus (0, \cdots, 0) \qquad \text{and} \qquad \mathbf{W}_{\mathbf{j}}^{\omega} = W_{j_1}^{\omega_1} \otimes \cdots \otimes W_{j_d}^{\omega_d}$$

where the spaces $W_{j_i}^{\omega_i}$ correspond to:

$$W_{j_i}^{\omega_i} = W_{j_i}^D \text{ if } \omega_i = 1, \quad W_{j_i}^{\omega_i} = V_{j_{min}}^D \text{ if } \omega_i = 0$$

Denoting by $\Psi_{\mathbf{j},\mathbf{k}}^{\omega}$ the wavelets of $\mathbf{W}_{\mathbf{j}}^{\omega}$, we define the curl-free wavelets and spaces by:

$$\Psi_{\mathbf{j},\mathbf{k}}^{\omega,\nabla} = \nabla\ [\Psi_{\mathbf{j},\mathbf{k}}^{\omega}] \qquad \text{and} \qquad \mathbf{W}_{\mathbf{j}}^{\omega,\nabla} = \text{span}\{\Psi_{\mathbf{j},\mathbf{k}}^{\omega,\nabla}\} \tag{32}$$

where $j_i \geq j_{min}$ and $0 \leq k_i \leq 2^j - 1$, for $1 \leq i \leq d$.

From proposition 1, the spaces spanned by these curl-free functions are contained in the following BMRA of $(L^2(\Omega))^d$:

$$\mathbf{V}_j^+ = \mathbf{V}_j^1 \times \cdots \times \mathbf{V}_j^d \quad \text{with} \quad \mathbf{V}_j^i = V_j^{1-\delta_{1,i}} \otimes \cdots \otimes V_j^{1-\delta_{d,i}}, \quad 1 \leq i \leq d$$

$\delta_{i,j}$ denotes the Kronecker symbol. This property allows fast coefficient computations on irrotational bases.

Since the spaces $\mathbf{V}_j$ defined in (29) constitute a multiresolution analysis of $H_0^1(\Omega)$, we get:

$$H_0^1(\Omega) = \mathbf{V}_{j_{min}} \bigoplus_{j_i \geq j_{min}} \left(\sum_{\omega \in \Omega_d^*} \mathbf{W}_{\mathbf{j}}^{\omega} \right), \quad 1 \leq i \leq d \tag{33}$$

Taking the gradient of relation (33) and using again proposition 1, we obtain:

$$\mathcal{H}_{curl}(\Omega) = \mathbf{V}^{\nabla}_{j_{min}} \bigoplus_{j_i \geq j_{min}} \left(\sum_{\omega \in \Omega^*_d} \mathbf{W}^{\omega,\nabla}_{\mathbf{j}} \right), \quad 1 \leq i \leq d \tag{34}$$

This relation (34) was proved in [18] in the case of 2D construction.

4 Wavelet Helmholtz-Hodge decomposition

4.1 Description of the method

The Helmholtz-Hodge decomposition, introduced in section 2, provides the orthogonal splitting of any vector field $\mathbf{u} \in (L^2(\Omega))^d$ into a divergence-free part, a curl-free part, and a gradient of a harmonic function:

$$\mathbf{u} = \mathbf{u}_{\text{div}} + \mathbf{u}_{\text{curl}} + \mathbf{u}_{\text{har}} \tag{35}$$

where:

$$\nabla \cdot \mathbf{u}_{\text{div}} = 0 \qquad \text{and} \qquad \mathbf{u}_{\text{div}} \cdot \mathbf{n} = 0$$

$$\nabla \times \mathbf{u}_{\text{curl}} = 0 \qquad \text{and} \qquad \mathbf{u}_{\text{curl}} \cdot \tau = 0$$

$$\nabla \times \mathbf{u}_{\text{har}} = 0 \qquad \text{and} \qquad \nabla \cdot \mathbf{u}_{\text{har}} = 0$$

$\mathbf{n}$ and τ are respectively the unit outward normal and tangent to the boundary $\partial\Omega$.

Our aim in this section is to describe a practical way to compute the components $\mathbf{u}_{\text{div}}$ and $\mathbf{u}_{\text{curl}}$ when $\Omega = [0,1]^3$. The most natural way, already followed in [23] for the Helmholtz decomposition, is to use the divergence-free and curl-free scaling functions and wavelet bases constructed in the previous section. Since $\mathcal{H}_{div}(\Omega) = \text{span}\{\Psi^{div}_{\mathbf{j},\mathbf{k}}\}$ and $\mathcal{H}_{curl}(\Omega) = \text{span}\{\Psi^{\nabla}_{\mathbf{j},\mathbf{k}}\}$ (we adopt a unified notation for the wavelet bases), the components $\mathbf{u}_{\text{div}}$ and $\mathbf{u}_{\text{curl}}$ are searched under the form of their wavelet series:

$$\mathbf{u}_{\text{div}} = \sum_{\mathbf{j},\mathbf{k}} d^{\text{div}}_{\mathbf{j},\mathbf{k}} \ \Psi^{div}_{\mathbf{j},\mathbf{k}} \qquad \text{and} \qquad \mathbf{u}_{\text{curl}} = \sum_{\mathbf{j},\mathbf{k}} d^{\nabla}_{\mathbf{j},\mathbf{k}} \ \Psi^{\nabla}_{\mathbf{j},\mathbf{k}} \tag{36}$$

By orthogonality of the decomposition (35) in $(L^2(\Omega))^d$, we obtain:

$$\langle \mathbf{u}, \Psi^{div}_{\mathbf{j},\mathbf{k}} \rangle = \langle \mathbf{u}_{\text{div}}, \Psi^{div}_{\mathbf{j},\mathbf{k}} \rangle \qquad \text{and} \qquad \langle \mathbf{u}, \Psi^{\nabla}_{\mathbf{j},\mathbf{k}} \rangle = \langle \mathbf{u}_{\text{curl}}, \Psi^{\nabla}_{\mathbf{j},\mathbf{k}} \rangle \tag{37}$$

Accordingly the computation of coefficients $(d^{\text{div}}_{\mathbf{j},\mathbf{k}})$ and $(d^{\nabla}_{\mathbf{j},\mathbf{k}})$ is reduced to the resolution of two linear systems:

$$\mathbb{M}_{\text{div}}(d^{\text{div}}_{\mathbf{j},\mathbf{k}}) = (\langle \mathbf{u}, \Psi^{div}_{\mathbf{j},\mathbf{k}} \rangle) \qquad \text{and} \qquad \mathbb{M}_{\text{curl}}(d^{\nabla}_{\mathbf{j},\mathbf{k}}) = (\langle \mathbf{u}, \Psi^{\nabla}_{\mathbf{j},\mathbf{k}} \rangle) \tag{38}$$

where $\mathbb{M}_{\text{div}}$ and $\mathbb{M}_{\text{curl}}$ are respectively the Gram matrices of the bases $\{\Psi^{div}_{\mathbf{j},\mathbf{k}}\}$ and $\{\Psi^{\nabla}_{\mathbf{j},\mathbf{k}}\}$.

The above method is nothing but orthogonal projections from $(L^2(\Omega))^d$ to $\mathcal{H}_{div}(\Omega)$ and $\mathcal{H}_{curl}(\Omega)$ respectively. In practice, $\mathbf{u}_{\text{div}}$ is searched as $\mathbf{u}^j_{\text{div}} \in \mathbf{V}^{div}_j$ for some j, and $\mathbf{u}_{\text{curl}}$ as $\mathbf{u}^j_{\text{curl}} \in \mathbf{V}^{curl}_j$. Then we recover from the usual Jackson-type estimations:

$$\forall\ \mathbf{u} \in \mathcal{H}_{div}(\Omega) \cap (H^s(\Omega))^d, \quad \|\mathbf{u} - \mathbf{u}^j_{\text{div}}\|_{(L^2(\Omega))^d} \leq C2^{-js}, \quad 0 \leq s \leq r-1$$

and

$$\forall\ \mathbf{u} \in \mathcal{H}_{curl}(\Omega) \cap (H^s(\Omega))^d, \quad \|\mathbf{u} - \mathbf{u}^j_{\text{curl}}\|_{(L^2(\Omega))^d} \leq C2^{-js}, \quad 0 \leq s \leq r-1$$

where r denotes the approximation order provided by the generator φ^1.

The last component $\mathbf{u}_{\text{har}}$ of the decomposition (35) is computed by subtracting $\mathbf{u}_{\text{div}}$ and $\mathbf{u}_{\text{curl}}$ from $\mathbf{u}$:

$$\mathbf{u}_{\text{har}} = \mathbf{u} - \mathbf{u}_{\text{div}} - \mathbf{u}_{\text{curl}} \tag{39}$$

4.2 Divergence-free and curl-free Gram matrices computation

In this section we present a practical computation of matrices $\mathbb{M}_{\text{div}}$ and $\mathbb{M}_{\text{curl}}$. For easy reading, we focus on the matrix $\mathbb{M}_{\text{curl}}$ in the 2D case. The extension to larger dimensions $d > 2$ follows readily from this two-dimensional case.

The key idea is to use the tensor structure of $\mathbb{M}_{\text{curl}}$ to reduce the computation. Let $\mathbf{M}_j$ and $\mathbf{R}_j$ denote respectively the Gram and stiffness matrices of the 1D basis $\{\psi^D_{j,k}\}$:

$$[\mathbf{M}_j]_{k,k'} = \langle \psi^D_{j,k}, \psi^D_{j,k'} \rangle \qquad \text{and} \qquad [\mathbf{R}_j]_{k,k'} = \langle (\psi^D_{j,k})', (\psi^D_{j,k'})' \rangle \tag{40}$$

The tensor structure of the basis $\{\Psi^{\nabla}_{\mathbf{j},\mathbf{k}}\}$ allows to express the inner product $\langle \Psi^{\nabla}_{\mathbf{j},\mathbf{k}}, \Psi^{\nabla}_{\mathbf{j}',\mathbf{k}'} \rangle$ in terms of matrix elements (40). By definition of the basis functions we get:

$$\langle \Psi^{\nabla}_{\mathbf{j},\mathbf{k}}, \Psi^{\nabla}_{\mathbf{j}',\mathbf{k}'} \rangle = \langle (\psi^D_{j_1,k_1})' \otimes \psi^D_{j_2,k_2}, (\psi^D_{j'_1,k'_1})' \otimes \psi^D_{j'_2,k'_2} \rangle + \langle \psi^D_{j_1,k_1} \otimes (\psi^D_{j_2,k_2})', \psi^D_{j'_1,k'_1} \otimes (\psi^D_{j'_2,k'_2})' \rangle$$

which rewrites:

$$\langle \Psi^{\nabla}_{\mathbf{j},\mathbf{k}}, \Psi^{\nabla}_{\mathbf{j}',\mathbf{k}'} \rangle = [\mathbf{M}_j]_{k_1,k'_1} \cdot [\mathbf{R}_j]_{k_2,k'_2} + [\mathbf{R}_j]_{k_1,k'_1} \cdot [\mathbf{M}_j]_{k_2,k'_2} \tag{41}$$

Then $\mathbb{M}_{\text{curl}}$ can be decomposed as:

$$\mathbb{M}_{\text{curl}} = \mathbf{M}_j \otimes \mathbf{R}_j + \mathbf{R}_j \otimes \mathbf{M}_j \tag{42}$$

The tensorial decomposition (42) has for main interest to reduce a 2D matrix-vector product with $\mathbb{M}_{\text{curl}}$ to matrix-matrix products with $\mathbf{M}_j$ and $\mathbf{R}_j$. More

precisely, if $(d^{\nabla}_{\mathbf{j},\mathbf{k}})$ denotes the vector of curl-free wavelet coefficients of $\mathbf{u}_{\text{curl}}$, defined in (36), equation (42) leads to:

$$[\mathbb{M}_{\text{curl}}(d^{\nabla}_{\mathbf{j},\mathbf{k}})] = \mathbf{M}_j[d^{\nabla}_{\mathbf{j},\mathbf{k}}]\mathbf{R}_j + \mathbf{R}_j[d^{\nabla}_{\mathbf{j},\mathbf{k}}]\mathbf{M}_j \tag{43}$$

where $[d^{\nabla}_{\mathbf{j},\mathbf{k}}]$ denotes the matrix of elements $d^{\nabla}_{\mathbf{j},\mathbf{k}}$. In practice the matrices only needed to compute and to store are the 1D matrices $\mathbf{M}_j$ and $\mathbf{R}_j$.

Finally, the matrix $\mathbb{M}_{\text{curl}}$ has a sparse structure, due to the compact support of basis functions. Figure 1 shows the shape of $\mathbb{M}_{\text{curl}}$, for $j = 6$, in the case of Daubechies generators with $r = 3$ vanishing moments. Remark that in 2D $\mathbb{M}_{\text{div}} = \mathbb{M}_{\text{curl}}$ (which is also the stiffness matrix of the Laplacian onto the wavelet basis $\{\psi^D_{j_1,k_1} \otimes \psi^D_{j_2,k_2}\}$), since we have:

$$\forall\ \mathbf{u}, \mathbf{v} \in H^1_0(\Omega);\quad \int_{\Omega} \mathbf{curl}(\mathbf{u}) \cdot \mathbf{curl}(\mathbf{v})\ dx\ =\ \int_{\Omega} \nabla\mathbf{u} \cdot \nabla\mathbf{v}\ dx \tag{44}$$

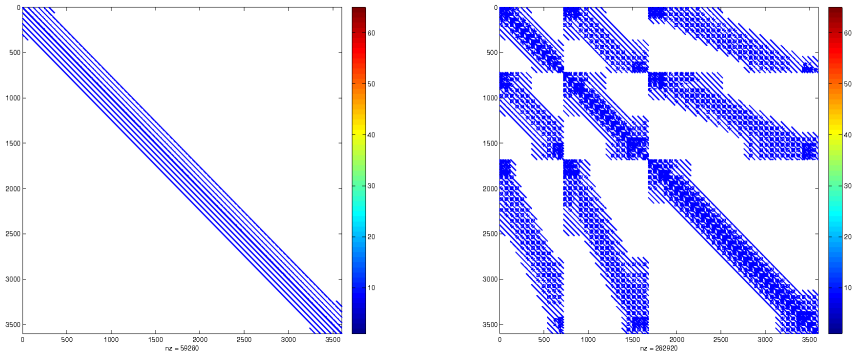

Fig. 1. Gram matrices of divergence-free scaling functions (left) and wavelets (right) built from Daubechies generators with $r = 3$, $j_{min} = 4$, $j = 6$.

4.3 Right-hand side computations

To solve system (38), we need to compute efficiently inner products $\langle \mathbf{u}, \Psi^{div}_{\mathbf{j},\mathbf{k}} \rangle$ and $\langle \mathbf{u}, \Psi^{\nabla}_{\mathbf{j},\mathbf{k}} \rangle$. This is achieved by using the decomposition of $\mathbf{u}$ in the wavelet bases in the suitable multiresolution analyses of $(L^2(\Omega))^d$ that contain alternatively the divergence-free or curl-free functions. To illustrate, we will explain the computation of $\langle \mathbf{u}, \Psi^{\nabla}_{\mathbf{j},\mathbf{k}} \rangle$ in the two dimensional case.

Let $(d^1_{\mathbf{j},\mathbf{k}})$ and $(d^2_{\mathbf{j},\mathbf{k}})$ denote respectively the coefficients of the decomposition of $\mathbf{u} = (\mathbf{u}_1, \mathbf{u}_2)$ on the wavelet basis of $(V_j^0 \otimes V_j^D) \times (V_j^D \otimes V_j^0)$:

$$\mathbf{u}_1 = \sum_{\mathbf{j},\mathbf{k}} d^1_{\mathbf{j},\mathbf{k}}\ \psi^0_{j_1,k_1} \otimes \psi^D_{j_2,k_2} \qquad \mathbf{u}_2 = \sum_{\mathbf{j},\mathbf{k}} d^2_{\mathbf{j},\mathbf{k}}\ \psi^D_{j_1,k_1} \otimes \psi^0_{j_2,k_2}$$

The computation of inner product $\langle \mathbf{u}, \Psi^{\nabla}_{\mathbf{j}',\mathbf{k}'} \rangle$ writes:

$$\begin{aligned}\langle \mathbf{u}, \Psi^{\nabla}_{\mathbf{j}',\mathbf{k}'} \rangle = &\sum_{\mathbf{j},\mathbf{k}} d^1_{\mathbf{j},\mathbf{k}}\ \langle \psi^0_{j_1,k_1} \otimes \psi^D_{j_2,k_2}, (\psi^D_{j_1',k_1'})' \otimes \psi^D_{j_2',k_2'} \rangle \\ &+ \sum_{\mathbf{j},\mathbf{k}} d^2_{\mathbf{j},\mathbf{k}}\ \langle \psi^D_{j_1,k_1} \otimes \psi^0_{j_2,k_2}, \psi^D_{j_1',k_1'} \otimes (\psi^D_{j_2',k_2'})' \rangle\end{aligned}$$

In terms of coefficient matrices $[d^1_{\mathbf{j},\mathbf{k}}]$ and $[d^1_{\mathbf{j},\mathbf{k}}]$, it becomes:

$$[\langle \mathbf{u}, \Psi^{\nabla}_{\mathbf{j}',\mathbf{k}'} \rangle] = \mathbf{C}_j^0\ [d^1_{\mathbf{j},\mathbf{k}}]\ \mathbf{M}_j + \mathbf{M}_j\ [d^2_{\mathbf{j},\mathbf{k}}]\ (\mathbf{C}_j^0)^t$$

where $\mathbf{C}_j^0$ is the stiffness matrix of elements: $\langle \psi^0_{j,k}, (\psi^D_{j',k'})' \rangle$. The computation of the Gram and stiffness matrices $\mathbf{M}_j$, $\mathbf{C}_j^0$ is classical [4] (see also [17,20]).

4.4 Divergence-free and curl-free Gram matrices preconditioning

The tensorial decomposition (42) of $\mathbb{M}_{\text{curl}}$ is used to deduce a preconditioner from those of matrices $\mathbf{M}_j \otimes \mathbf{R}_j$ and $\mathbf{R}_j \otimes \mathbf{M}_j$. Let $\mathbf{I}_j$ be the identity matrix of dimension $(N_j - 2)$ and $\mathbf{I}_R$ be the diagonal matrix of $\mathbf{R}_j$:

$$[\mathbf{I}_j]_{k,k'} = \delta_{k,k'} \qquad \text{and} \qquad [\mathbf{I}_R]_{k,k'} = [\mathbf{R}_j]_{k,k'}\delta_{k,k'}, \quad 1 \le k, k' \le N_j - 2$$

On one hand, as an optimal (and diagonal) preconditioner of $\mathbf{R}_j$ is given by the inverse of $\mathbf{I}_R$ (see [7,10]), readily we deduce optimal diagonal preconditioners of matrices $\mathbf{M}_j \otimes \mathbf{R}_j$ and $\mathbf{R}_j \otimes \mathbf{M}_j$ by respectively the inverse of matrices $\mathbf{I}_j \otimes \mathbf{I_R}$ and $\mathbf{I_R} \otimes \mathbf{I}_j$.

On the other hand, since $\mathbb{M}_{\text{curl}}$ is the 2D stiffness matrix of a scalar Laplacian on the basis $\{\psi^D_{j_1,k_1} \otimes \psi^D_{j_2,k_2}\}$, an optimal preconditioner is given by the inverse of its diagonal matrix [7,10]. Then, the inverse of the diagonal matrix $\mathbf{D}_j$ defined by:

$$\mathbf{D}_j = \mathbf{I}_j \otimes \mathbf{I_R} + \mathbf{I_R} \otimes \mathbf{I}_j$$

is an optimal diagonal preconditioner for $\mathbb{M}_{\text{curl}}$.

However, the matrix $\mathbf{D}_j$ has the same size as $\mathbb{M}_{\text{curl}}$. To reduce the complexity, we replace the 2D matrix-vector product $\mathbf{D}_j(d^{\nabla}_{\mathbf{j},\mathbf{k}})$ by the following matrix-matrix products:

$$[\mathbf{D}_j(d^{\nabla}_{\mathbf{j},\mathbf{k}})] = [d^{\nabla}_{\mathbf{j},\mathbf{k}}]\mathbf{I_R} + \mathbf{I_R}[d^{\nabla}_{\mathbf{j},\mathbf{k}}] \tag{45}$$

Because of the diagonal structure of $\mathbf{I_R}$, equation (45) is then reduced to term by term matrix product:

$$[\mathbf{D}_j(d^{\nabla}_{\mathbf{j},\mathbf{k}})]_{k,k'} = [d^{\nabla}_{\mathbf{j},\mathbf{k}}]_{k,k'} \cdot [\mathbf{I}^*_{\mathbf{R}}]_{k,k'} \quad \text{where} \quad [\mathbf{I}^*_{\mathbf{R}}]_{k,k'} = [\mathbf{I_R}]_{k,k} + [\mathbf{I_R}]_{k',k'} \tag{46}$$

From equation (46), multiplying $(d^{\nabla}_{\mathbf{j},\mathbf{k}})$ by the matrix $\mathbf{D}_j^{-1}$ is therefore equivalent to divide term by term the matrix $[d^{\nabla}_{\mathbf{j},\mathbf{k}}]$ by $\mathbf{I}^*_{\mathbf{R}}$.

The preconditioner $\mathbf{I}^*_{\mathbf{R}}$ is also valid for the matrix $\mathbb{M}_{\text{div}}$ in dimension two ($d = 2$) since $\mathbb{M}_{\text{div}} = \mathbb{M}_{\text{curl}}$.

The performance of the above preconditioner for $\mathbb{M}_{\text{curl}}$ was tested in two and three dimensions, using a preconditioned conjugate gradient method to solve system (43), with a random right hand side. Then we study the number of iterations needed to reach a given residual, first with respect to the dimension index j, second with respect to the regularity (approximation order r) of the basis functions. Figure 2 shows that the number of iterations does not increase significantly with the dimension index j, in the periodic and non periodic cases, which indicates that our preconditioner is quasi-optimal.

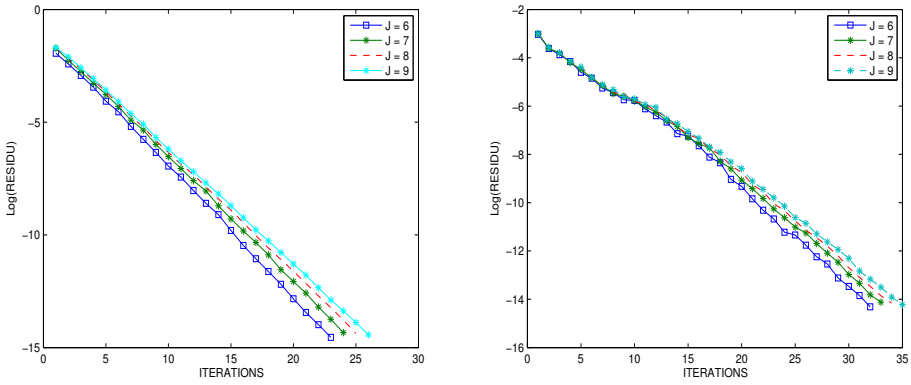

Fig. 2. Preconditioned conjugate gradient residual versus iteration number, for different values of the dimension index j: periodic case (left) and non periodic case (right). Daubechies generators ψ^1 with $r = 3$ vanishing moments, $j_{min} = 3$ in non periodic (2D case).

Figure 3 (two-dimensional case) and figure 4 (three-dimensional case) highlight that the approximation order r speed up the convergence of the resolution. The behaviour of the slopes are less regular in the non periodic case, because of the influence of the smallest scale $j_{min} > 0$ (see [10] for similar conclusions).

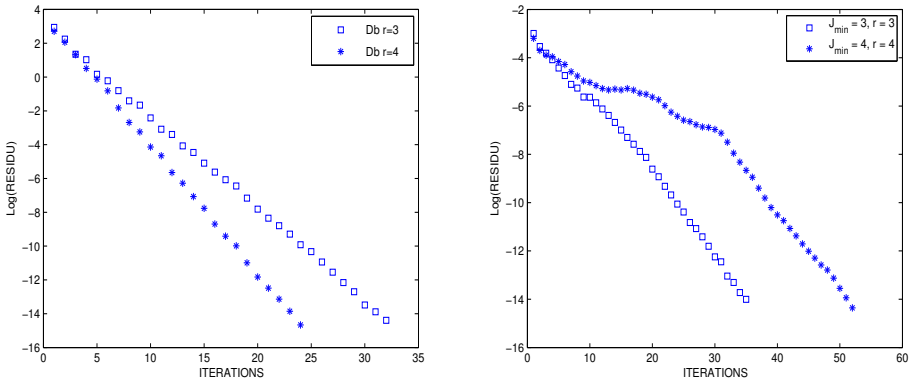

Fig. 3. Preconditioned conjugate gradient residuals versus iteration number, for different values of the approximation order r: periodic case (left) and non periodic case (right). Daubechies generators ψ^1 with $r = 3$ and $r = 4$ vanishing moments. The resolution is $j = 10$ in two dimension ($d = 2$).

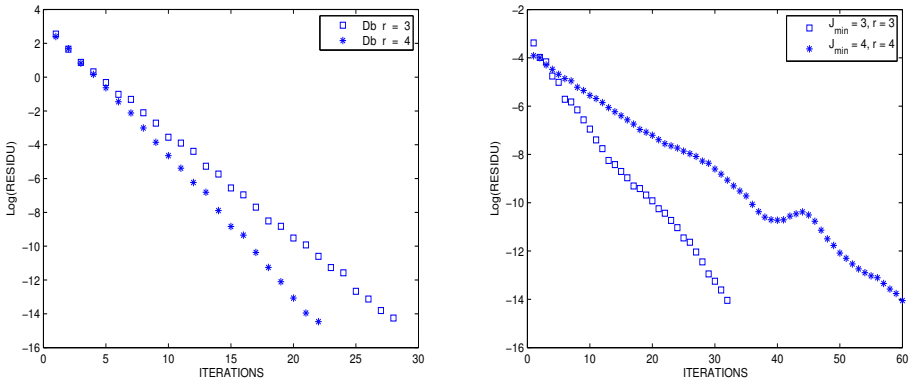

Fig. 4. Preconditioned conjugate gradient residuals versus iteration number, for different values of the approximation order r: periodic case (left) and non periodic case (right). Daubechies generators ψ^1 with $r = 3$ and $r = 4$ vanishing moments. The resolution is $j = 7$ in three dimension ($d = 3$).

4.5 Examples of Helmholtz-Hodge and Helmholtz decomposition

In this section, we carry out some experiments to illustrate and study the convergence rate of the Helmholtz-Hodge decomposition. First we show in dimension two, the Helmholtz decomposition of a vector field $\mathbf{u}$ (Figure 5), and its Helmholtz-Hodge decomposition (Figure 7). The vector field $\mathbf{u}$ was constructed

analytically:

$$\mathbf{u}_{2D} = \mathbf{u}_{\text{div}} + \mathbf{u}_{\text{curl}} + \mathbf{u}_{\text{har}}$$

where:

$$\mathbf{u}_{\text{div}} = \begin{vmatrix} \sin(2\pi x)^2 \sin(4\pi y) \\ -\sin(4\pi x)\sin(2\pi y)^2 \end{vmatrix}, \ \mathbf{u}_{\text{curl}} = \begin{vmatrix} \sin(4\pi x)\sin(2\pi y)^2 \\ \sin(2\pi x)^2 \sin(4\pi y) \end{vmatrix}, \ \mathbf{u}_{\text{har}} = (1/2, -1/4)$$

The terms of the decompositions are computed using the method described previoulsy.

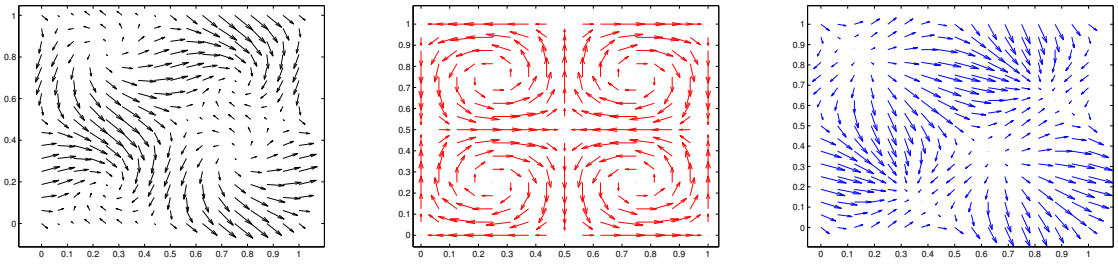

(a) Initial vector field $\mathbf{u}^j_{2D}$ (b) Divergence-free part $\mathbf{u}^j_{\text{div}}$ (c) Curl-free part $\mathbf{u}^j_{\text{curl}} + \mathbf{u}^j_{\text{har}}$

Fig. 5. Example of Helmholtz decomposition.

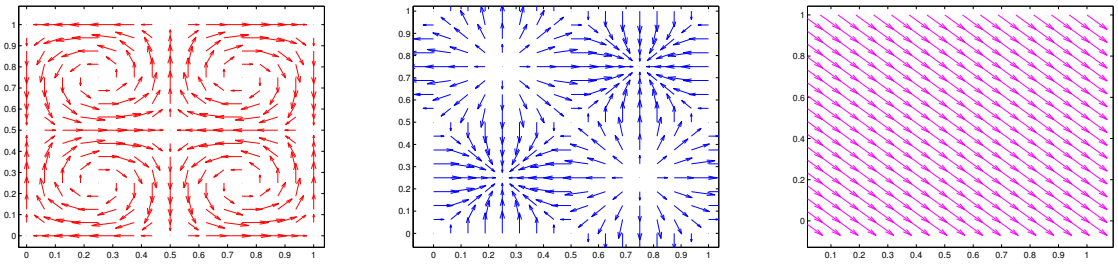

(a) Divergence-free part $\mathbf{u}^j_{\text{div}}$ (b) Curl-free part $\mathbf{u}^j_{\text{curl}}$ (c) Gradient of harmonic part $\mathbf{u}^j_{\text{har}}$

Fig. 6. Example of Helmholtz-Hodge decomposition.

Then we investigate the convergence rate of the projection error onto the divergence-free vector space $\mathbf{V}^{div}_j$, in two and three dimensions. The tests have

been performed on analytic fields, which we know the exact solutions. We used $\mathbf{u}_{2D}$ in two dimensions and $\mathbf{u}_{3D}$ in three dimensions:

$$\mathbf{u}_{3D} = \begin{vmatrix} \sin(2\pi x)^2 \sin(4\pi y) \sin(4\pi z) + \sin(4\pi x) \sin(2\pi y)^2 \sin(2\pi z)^2 \\ \sin(4\pi x) \sin(2\pi y)^2 \sin(4\pi z) + \sin(2\pi x)^2 \sin(4\pi y) \sin(2\pi z)^2 \\ -2 \sin(4\pi x) \sin(4\pi y) \sin(2\pi z)^2 + \sin(2\pi x)^2 \sin(2\pi y)^2 \sin(4\pi z) \end{vmatrix} \tag{47}$$

The solutions verify homogeneous Dirichlet boundary conditions by construction. Figure 7 plot the ℓ_2-projection errors in terms of the dimension index j with generators of approximation order $r = 3$. For both experiments (2D and 3D), the convergence rate follows the theoretical law of -2 predicted in (11).

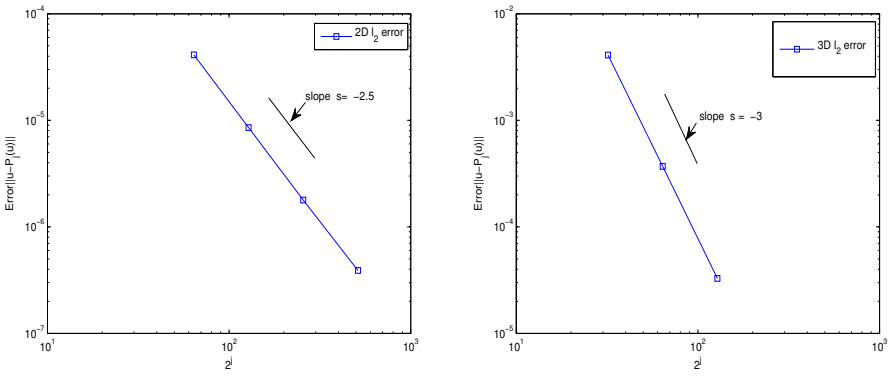

Fig. 7. ℓ_2-projection error onto $\mathbf{V}_j^{div}$ versus j. Two-dimensional case (left) and three-dimensional case (right). The generators $(\varphi^1, \tilde{\varphi}^1)$ correspond to biorthogonal splines with: $r = \tilde{r} = 3$.

5 Conclusion

In this paper, we have presented a practical algorithm to compute the Helmholtz-Hodge decomposition of a vector field in the hypercube. Our method is based on the existence of divergence-free and irrotational wavelet bases satisfying boundary conditions. After presenting the principles of their construction in any dimension, we have detailed the computation of each term of the decomposition, which requires the inversion of divergence-free and curl-free wavelet Gram matrices. We have used the tensorial structure of the bases to propose an optimal and diagonal preconditioning, to invert the system using a preconditioned conjugate gradient. Numerical tests on 2D and 3D analytical vector fields illustrate the potential of the approach, in terms of complexity and storage.
Since the Helmholtz-Hodge decomposition is a key ingredient for the analysis

and simulation of incompressible flows, future works will present its application in numerical schemes for the Stokes and Navier-Stokes equations [17].

References

1. Amrouche, C., Bernardi, C., Dauge, M., Girault, V.: Vector potentials in three dimensional nonsmooth domains. Math. Meth. in the Applied Sciences 21, 823–864 (1998)
2. Amrouche, C., Seloula, N.: L^p-theory for vector potentials and Sobolev's inequalities for vector fields. C. R. Acad. Sci. Paris Ser. I 349, 529–534 (2011)
3. Battle, G., Federbush, P.: Divergence-free vector wavelets. Michigan Math. Journ. 40, 181-195 (1993)
4. Beylkin, G.: On the representation of operator in bases of compactly supported wavelets. SIAM J. Numer. Anal. 6, 1716–1740 (1992)
5. Chiavassa, G., Liandrat, J.: On the Effective Construction of Compactly Supported Wavelets Satisfying Homogeneous Boundary Conditions on the Interval. Appl. Comput. Harmon. Anal. 4, 62–73 (1997)
6. Chorin, A., Marsden, J.: A Mathematical Introduction to Fluid Mechanics. Springer, (1992)
7. Cohen, A.: Numerical Analysis of Wavelet Methods. Elsevier, (2003)
8. Cohen, A., Daubechies, I., Feauveau, J.-C.: Biorthogonal bases of compactly supported wavelets. Comm. Pure Appli. Maths. 45, 485–560 (1992)
9. Cohen, A., Daubechies, I., Vial, P.: Wavelets on the Interval and Fast Wavelet Transforms. Appl. Comput. Harmon. Anal. 1, 54–81 (1993)
10. Cohen, A., Masson, R: Wavelet Methods for Second-Order Elliptic Problems, Preconditioning, and Adaptivity. SIAM J. on Sci. Comput. 21, 1006–1026 (1999)
11. Deriaz, E., Perrier, V.: Orthogonal Helmholtz decomposition in arbitrary dimension using divergence-free and curl-free wavelets. Appl. Comput. Harmon. Anal. 26, 249–269 (2009)
12. Deriaz, E., Perrier, V.: Divergence-free and curl-free wavelets in 2D and 3D, application to turbulent flows. J. of Turbulence 7, 1–37 (2006)
13. Dodu, F., Rabut, C.: Irrotational or Divergence-Free Interpolation. Numerisch Mathematic 98, 477–498 (2004)
14. Girault, V., Raviart, P.A.: Finite element methods for Navier-Stokes equations. Springer, Verlag Berlin (1986)
15. Grivet-Talocia, S., Tabacco, A.: Wavelet on the interval with optimal localization. Math. Models. Meth. Appl. Sci. 10, 441–462 (2000)
16. Jouini, A., Lemarié-Rieusset, P.G.: Analyse multirésolution biorthogonale sur l'intervalle et applications. Annales de l'I.H.P. Section C 10, 453–476 (1993)
17. Kadri-Harouna, S.: Ondelettes pour la prise en compte de conditions aux limites en turbulence incompressible. Phd thesis of Grenoble University (2010)
18. Kadri-Harouna, S., Perrier, V.: Divergence-free and Curl-free Wavelets on the Square for Numerical Simulation. Preprint hal-00558474 (2010)
19. Lemarié-Rieusset, P.G.: Analyses multi-résolutions non orthogonales, commutation entre projecteurs et dérivation et ondelettes vecteurs à divergence nulle. Revista Matemática Iberoamericana 8, 221–236 (1992)
20. Monasse, P., Perrier, V.: Orthogonal Wavelet Bases Adapted For Partial Differential Equations With Boundary Conditions. SIAM J. Math. Anal. 29, 1040–1065 (1998)

21. Petronetto, F., Paiva, A., Lage, M., Tavares, G., Lopes, H., Lewiner, T.: Meshless Helmholtz-Hodge decomposition. IEEE Trans. on Visu. and Comp. Graps. 16, 338–342 (2010)
22. Polthier, K., Preub, E.: Identifying Vector Field Singularities using a Discrete Hodge Decomposition. In: Visualization and Mathematics III, Eds: H.C. Hege, K. Polthier, 113-134. Springer Verlag (2003)
23. Stevenson, R.: Divergence-free wavelet bases on the hypercube. Appl. Comput. Harmon. Anal. 30, 1–19 (2011)
24. Stevenson, R.: Divergence-free wavelet bases on the hypercube: Free-slip boundary conditions, and applications for solving the instationary Stokes equations. Math. Comp. 80, 1499-1523 (2011)
25. Tong, T., Lombeyda, S., Hirani, A.N., Desbrun, M.: Discrete multiscale vector field decomposition. ACM Transactions on Graphics (TOG) 22, 445–452 (2003)
26. Urban, K.: Wavelet Bases in H(div) and H($curl$). Math. Comput. 70, 739–766 (2000)
27. Urban, K.: Wavelets in Numerical Simulation. Springer, Berlin (2002)